Cell Stem Cell
Article

The PSA$^{-/lo}$ Prostate Cancer Cell Population Harbors Self-Renewing Long-Term Tumor-Propagating Cells that Resist Castration

Jichao Qin,[1,2,12] Xin Liu,[1,3,12] Brian Laffin,[1] Xin Chen,[1,4] Grace Choy,[1] Collene R. Jeter,[1] Tammy Calhoun-Davis,[1] Hangwen Li,[1,3] Ganesh S. Palapattu,[5] Shen Pang,[6] Kevin Lin,[1] Jiaoti Huang,[7] Ivan Ivanov,[8] Wei Li,[9] Mahipal V. Suraneni,[1] and Dean G. Tang[1,4,10,11,*]

[1]Department of Molecular Carcinogenesis, University of Texas M.D. Anderson Cancer Center, Science Park, Smithville, TX 78957, USA
[2]Department of Surgery, Tongji Hospital, Tongji Medical College, Huazhong University of Science and Technology, Wuhan 430030, China
[3]Department of Nutritional Science, University of Texas at Austin, Austin, TX 78712, USA
[4]Program in Molecular Carcinogenesis, University of Texas Graduate School of Biomedical Sciences, Houston, TX 77030, USA
[5]Department of Urology, The Methodist Hospital, Houston, TX 77030, USA
[6]UCLA Dental Research Institute and UCLA School of Dentistry, 10833 Le Conte Avenue, Los Angeles, CA 90095, USA
[7]Department of Pathology and Laboratory Medicine, David Geffen School of Medicine, UCLA, Los Angeles, CA 90095, USA
[8]Department of Veterinary Physiology and Pharmacology, Texas A&M University, College Station, TX 77843, USA
[9]Department of Molecular and Cellular Biology, Baylor College of Medicine, Houston, TX 77030, USA
[10]Centers for Cancer Epigenetics, Stem Cell and Developmental Biology, RNA Interference and Non-coding RNAs, and Molecular Carcinogenesis, University of Texas M.D. Anderson Cancer Center, Houston, TX 77030, USA
[11]Cancer Stem Cell Institute, Research Center for Translational Medicine, East Hospital, Tongji University, Shanghai 200120, China
[12]These authors contributed equally to this work
*Correspondence: dtang@mdanderson.org
DOI 10.1016/j.stem.2012.03.009

SUMMARY

Prostate cancer (PCa) is heterogeneous and contains both differentiated and undifferentiated tumor cells, but the relative functional contribution of these two cell populations remains unclear. Here we report distinct molecular, cellular, and tumor-propagating properties of PCa cells that express high (PSA$^+$) and low (PSA$^{-/lo}$) levels of the differentiation marker PSA. PSA$^{-/lo}$ PCa cells are quiescent and refractory to stresses including androgen deprivation, exhibit high clonogenic potential, and possess long-term tumor-propagating capacity. They preferentially express stem cell genes and can undergo asymmetric cell division to generate PSA$^+$ cells. Importantly, PSA$^{-/lo}$ PCa cells can initiate robust tumor development and resist androgen ablation in castrated hosts, and they harbor highly tumorigenic castration-resistant PCa cells that can be prospectively enriched using ALDH$^+$CD44$^+\alpha2\beta1^+$ phenotype. In contrast, PSA$^+$ PCa cells possess more limited tumor-propagating capacity, undergo symmetric division, and are sensitive to castration. Altogether, our study suggests that PSA$^{-/lo}$ cells may represent a critical source of castration-resistant PCa cells.

INTRODUCTION

Prostate cancer (PCa) is heterogeneous, manifesting variegated cellular morphologies and histopathological presentations. PCa also exhibits great intratumor histological and immunophenotypic heterogeneities, with low-grade tumors often harboring poorly differentiated areas and high-grade tumors containing relatively differentiated foci. The cellular basis for the histological and cellular heterogeneity of PCa remains unclear.

Androgen and androgen receptor (AR) signaling has been implicated in PCa. Androgen-deprivation therapy (ADT) blocks androgen production or AR signaling and is the mainstay treatment for advanced and recurrent PCa, but such interventions only achieve short-term efficacy due to the emergence of castration-resistant disease (i.e., castration-resistant prostate cancer, CRPC). Although many mechanisms, mostly centered on AR, have been proposed for CRPC development (Shen and Abate-Shen, 2010; Wang et al., 2009a), the cell-of-origin and molecular identity of CRPC cells remain undefined.

Numerous studies have demonstrated that prostate-specific antigen (PSA) protein expression in PCa positively correlates with its overall degree of differentiation (e.g., Abrahamsson et al., 1988; Feiner and Gonzalez, 1986; Gallee et al., 1990). At the cellular level, PCa contains differentiated cancer cells expressing high levels of PSA (i.e., PSA$^+$), as well as PCa cells that express little or no PSA (i.e., PSA$^{-/lo}$). The PSA$^{-/lo}$ cells appear to be rare in early-stage tumors but become more abundant in high-grade and locally advanced tumors, and some cases of PCa may completely lack PSA expression. PCa patients with tumors containing >50% PSA$^+$ PCa cells tend to have longer survival (Roudier et al., 2003; Shah et al., 2004). These clinical observations raise a fundamental question: could PSA$^{-/lo}$ PCa cells be intrinsically distinct from PSA$^+$ cells and thus play differential roles in tumor maintenance and progression to CRPC? Herein, we address this clinically relevant question using a PSA promoter-driven lentiviral reporter system to separate bulk PCa cells into PSA$^{-/lo}$ and PSA$^+$ subpopulations.

RESULTS

Increased PSA$^{-/lo}$ Cells and Reduced *PSA* mRNA in High-Grade Primary Tumors and Recurrent PCa

We first performed a semiquantitative PSA immunohistochemical (IHC) analysis in cohorts of untreated Gleason 7 (GS7, n = 10), Gleason 9 or 10 (GS9/10, n = 10), and treatment-failed (n = 23) PCa (see Figure S1 and Table S1 available online). Most tumor glands in GS7 tumors stained strongly for PSA, but there existed poorly differentiated areas of PSA$^{-/lo}$ cells (Figure S1A). In contrast, in GS9/10 tumors, the main histological pattern was undifferentiated tumor mass in which most tumor cells were PSA$^{-/lo}$, with PSA^{+} foci only occasionally present (Figure S1B). In 23 recurrent PCa cases (mainly CRPC), some tumors resembled untreated GS9/10 tumors, but most tumors completely lacked PSA^{+} PCa cells (Figures S1C–S1F). Quantification revealed significantly increased numbers of PSA$^{-/lo}$ PCa cells in untreated GS9/10 and treatment-failed PCa compared to untreated GS7 tumors (Figure 1A).

Consistent with the IHC results, analysis of multiple microarray data sets in *Oncomine* revealed that tumor *PSA* mRNA levels were significantly decreased in high-grade primary tumors and in recurrent and metastatic PCa (Figure S2; data not shown). Importantly, reduced tumor *PSA* mRNA levels correlated with lymph node positivity, tumor recurrence, metastasis, and shortened patient survival (Figure S2; data not shown; see also Figure 6A). Together, the PSA IHC and mRNA analysis indicates that advanced and recurrent PCa have lower *PSA* mRNA and more undifferentiated PSA$^{-/lo}$ cells.

A Lentiviral Reporter System that Separates PSA$^{-/lo}$ PCa Cells from PSA^{+} Cells

To separate PSA$^{-/lo}$ from PSA^{+} PCa cells, we employed the PSAP-GFP lentivector, in which the PSA promoter (PSAP) drives eGFP expression (Yu et al., 2001) (Figure S3A). The PSAP was originally isolated from a PCa patient with high-serum PSA and was highly specific and sensitive for PSA-positive prostate (cancer) cells. We also generated two modified PSAP-GFP vectors (Figure S3A).

Using the PSAP-GFP vector, we infected LNCaP cells at an multiplicity of infection (MOI) of 25 (Figure 1B), at which virtually all cells were infected, as evidenced by PCR detection of the GFP sequence in genomic DNA of randomly picked clones (Figure 1C). We then used fluorescence-activated cell sorting (FACS) to purify out the top 10% GFP-bright (GFP^{+}) and bottom 2%–6% GFP-negative/GFP-dim (i.e., GFP$^{-/lo}$) LNCaP cells. The purity of GFP$^{-/lo}$ and GFP^{+} cells was 98%–100% and ≥97%, respectively (e.g., Figure S3B). LNCaP cells routinely cultured in RPMI-7% fetal bovine serum (FBS) contained 2.7% ± 1.8% (0.3%–6.0%; n = 15) GFP$^{-/lo}$ cells. When LNCaP cells were infected with PSAP-GFP-Psv40-neo (Figure S3A) followed by G418 selection for several weeks, we observed 2.7% ± 1.7% (n = 7) GFP$^{-/lo}$ cells.

The percentage of GFP$^{-/lo}$ LNCaP cells was very close to that of PSA$^{-/lo}$ cells in LNCaP cultures (2.2% ± 1.5%; n = 4). Real-time (qPCR; Figure 1D) and semiquantitative (Figure S3C) RT-PCR revealed lower *PSA* mRNA levels in GFP$^{-/lo}$ LNCaP cells compared to the corresponding GFP^{+} cells. Also, most purified GFP^{+} LNCaP cells stained strongly positive for PSA protein, whereas GFP$^{-/lo}$ cells were weak or negative for PSA (Figure 1E). GFP$^{-/lo}$ LNCaP cells also expressed lower levels of AR mRNA (Figure 1D; Figure S3C) and protein (Figures 1F and 1G) compared to GFP^{+} cells. These results indicate that the PSAP-GFP lentiviral system faithfully reports endogenous PSA expression. Hence, in many forgoing experiments we refer to GFP^{+} and GFP$^{-/lo}$ cells as PSA^{+} and PSA$^{-/lo}$ cells, respectively.

AR staining revealed ~82% and 18% GFP^{+} LNCaP cells showing strong and intermediate nuclear AR, respectively, and no GFP^{+} LNCaP cells were negative for AR (Figure 1F). In contrast, 46% of the PSA$^{-/lo}$ LNCaP cells were completely negative for AR, whereas 41% and 13% PSA$^{-/lo}$ LNCaP cells had weak and strong AR, respectively (Figure 1F). These results suggest that the majority of PSA^{+} PCa cells are high in AR, whereas PSA$^{-/lo}$ cells express a gradient of AR, from completely negative to strong nuclear staining.

PSA$^{-/lo}$ LNCaP Cells Preferentially Express Antistress Genes and Are Resistant to Androgen Deprivation, Chemotherapeutics, and Pro-Oxidants

When PSAP-GFP-infected LNCaP cells were cultured in androgen-deprived conditions, i.e., using charcoal dextran-stripped serum (CDSS) or with bicalutamide (an antiandrogen), PSA^{+} cells dramatically decreased with a concomitant expansion of PSA$^{-/lo}$ cells (Figure S3D). Purified PSA$^{-/lo}$ LNCaP cells also displayed higher survival and holoclone-forming (Li et al., 2008) capacity in the absence of androgen (Figure S3E). These results suggest that PSA$^{-/lo}$ PCa cells are resistant to androgen deprivation.

Whole-genome transcriptome profiling in purified PSA$^{-/lo}$ and PSA^{+} LNCaP cells revealed distinct gene expression patterns in the two isogenic subpopulations (Figure 1H). A total of 726 probes representing 561 unique genes was significantly overexpressed, whereas 557 probes representing 403 genes were underexpressed (fold change [FC] ≥ 1.4, $p < 0.05$) in PSA$^{-/lo}$ LNCaP cells (Figure S3F; Figure S3G shows qPCR of several genes). A combination of Gene Ontology (GO) analysis and literature-based curation put many of these differentially expressed genes into distinct functional categories (Figure 1H; Table S2). Strikingly, as many as 10% of the genes overexpressed in PSA$^{-/lo}$ LNCaP cells were involved in antistress responses, which included detoxification (metallothioneins, GSTT2, etc.), hypoxia-responsive (HIF1α, THBS1, PLAU, APLN), p53 signaling (e.g, ZBTB7A, PSME3), and DNA-damage sensing/repair (e.g., MSH6, XPA, REV1) genes (Figures 1H and 1I; Table S2). The PSA$^{-/lo}$ LNCaP cells also overexpressed Bcl-2 and underexpressed many proapoptotic genes (Table S2).

Differential expression of antistress and proapoptotic genes suggests that the PSA$^{-/lo}$ cells would be more resistant to not only androgen deprivation but also other stresses. Indeed, when LNCaP cells infected with PSAP-GFP were treated with CDSS plus bicalutamide, etoposide, paclitaxel (taxol), or H_2O_2, PSA$^{-/lo}$ cells expanded with concomitant decreases in PSA^{+} cells (Figure 1J). FACS analysis indicated that these treatments preferentially induced apoptosis in PSA^{+} LNCaP cells (data not shown).

PSA$^{-/lo}$ LNCaP Cells Underexpress Genes Associated with Cell-Cycle Progression and Mitosis, Are Quiescent, and Possess Stem Cell Gene Expression Profiles

The PSA$^{-/lo}$ LNCaP cells underexpressed dozens of cell-cycle and mitosis-related genes (Figure 1H; Figure S3H; Table S2),

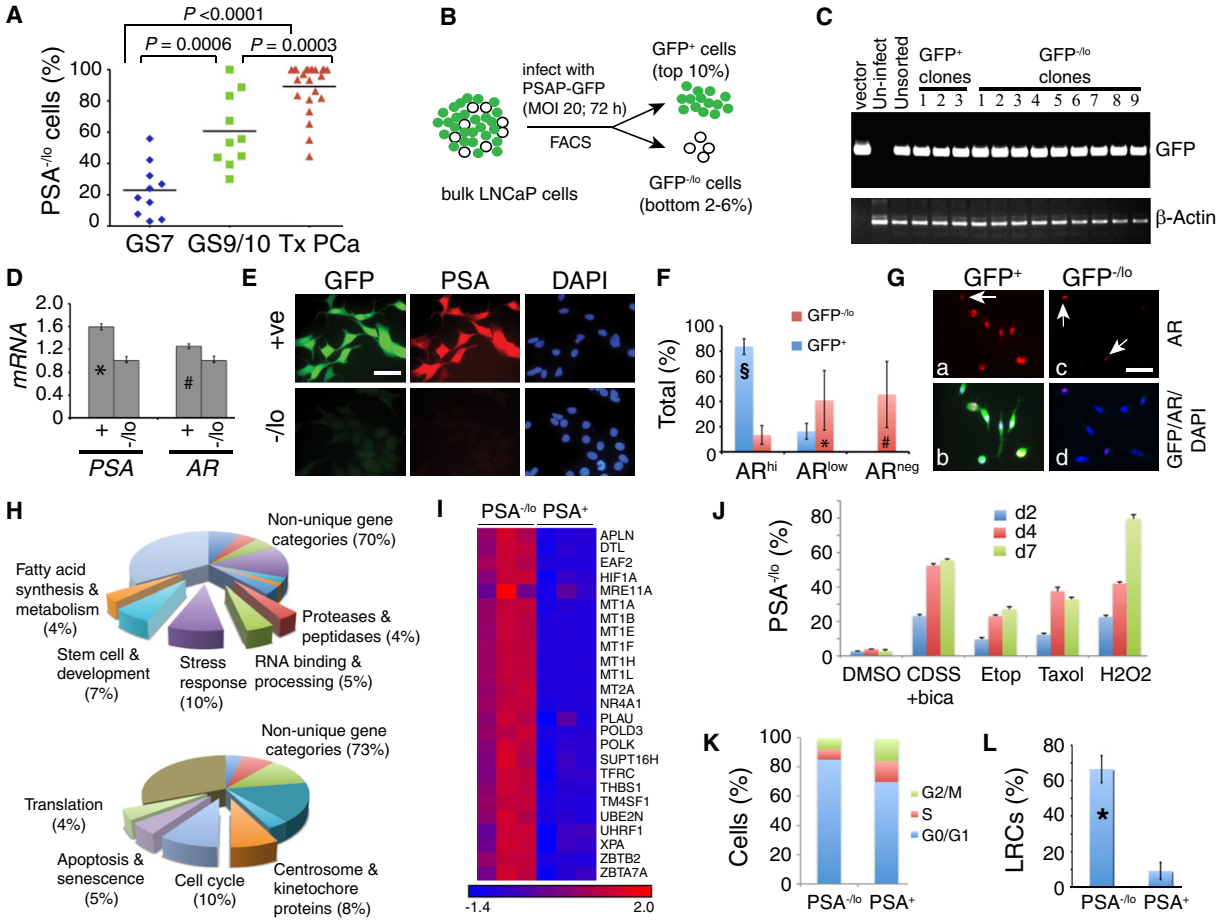

Figure 1. Distinct Molecular and Biological Properties of PSA$^{-/lo}$ and PSA^{+} LNCaP Cells

(A) Abundance of PSA$^{-/lo}$ tumor cells in untreated low-grade (GS7) and high-grade (GS9/10) tumors or in treatment-failed (Tx) PCa. See Table S1 and Figure S1 for relevant information.

(B) Schematic of GFP^{+} and GFP$^{-/lo}$ cell sorting.

(C) Genomic PCR of GFP sequence in clonally derived LNCaP cells. β-actin, control for DNA; PSAP-GFP vector, positive control for GFP. Shown are results from 3 GFP^{+} and 9 GFP$^{-/lo}$ (1–3, type I; 4–6, type II; 7–9, type III; see Figure S4F for clone types) clones.

(D) qPCR analysis of *PSA* and *AR* mRNA in GFP^{+} and GFP$^{-/lo}$ LNCaP cells (n = 3; all error bars in all figures represent the mean ± SD unless otherwise stated). *p = 0.005; #p = 0.047.

(E) Representative microphotographs (scale bar represents 20 μm) of PSA staining in GFP^{+} and GFP$^{-/lo}$ LNCaP cells (n = 4).

(F and G) GFP$^{-/lo}$ LNCaP cells express lower levels of nuclear AR. (F) Cells that expressed high (AR^{hi}), low (AR^{low}), and no (AR^{neg}) nuclear AR were counted, and the results were expressed as percentage of total (mean ± S.D; §p = 6.97E09; *p = 0.05; #p = 0.008). (G) Representative images (scale bar represents 20 μm). In (Ga) and (Gb), all cells are AR^{hi}, with only one AR^{low} (arrow) cell. In (Gc) and (Gd), all cells are AR^{neg}, with two cells being AR^{low} (arrows).

(H) Distinct gene expression profiles of PSA$^{-/lo}$ and PSA^{+} LNCaP cells. Shown are pie charts of gene categories (percentage indicated) overexpressed (top) and underexpressed (bottom) in PSA$^{-/lo}$ cells.

(I) Heat map presentation of representative antistress genes overexpressed in PSA$^{-/lo}$ LNCaP cells. The scale bar depicts relative expression levels (log scale) derived from raw values of each gene divided by its respective SD across all six samples and centered at 0.

(J) PSA$^{-/lo}$ LNCaP cells are resistant to androgen deprivation (i.e., CDSS plus bicalutamide), as well as chemotherapeutics and hydrogen peroxide. Shown are % PSA$^{-/lo}$ cells in PSAP-GFP-infected LNCaP cells treated with the conditions indicated for 2, 4, and 7 days (d). Differences between all individual treatments and DMSO are statistically significant ($p < 0.01$; mean ± SD; n = 4).

(K) PSA$^{-/lo}$ LNCaP cells are slow cycling. Cell-cycle analysis in purified PSA$^{-/lo}$ versus PSA^{+} LNCaP cells. Shown are the mean percentages of cells in different phases of the cell cycle (n = 2).

(L) PSA$^{-/lo}$ LNCaP cells are quiescent. Shown is the percent label (i.e., BrdU) of retaining cells (LRCs) in purified PSA$^{-/lo}$ versus PSA^{+} LNCaP cells (mean ± SD; n = 3). *$p < 0.0001$.

suggesting that PSA$^{-/lo}$ PCa cells may be more quiescent than PSA^{+} cells. Several lines of evidence supported this suggestion. First, cell-cycle analysis revealed a smaller percentage of PSA$^{-/lo}$ LNCaP cells in S and G2/M phases (Figure 1K). Second, the PSA$^{-/lo}$ and PSA^{+} LNCaP populations had 4.2% and 12%, respectively, of Ki-67^{+} cells ($p < 0.0001$). Third, BrdU label-retaining experiments demonstrated that many more PSA$^{-/lo}$ LNCaP cells retained the BrdU label upon an 11-d chase (Figure 1L).

The observations that PSA$^{-/lo}$ LNCaP cells are quiescent and resist stress stimulations suggest that the population may be

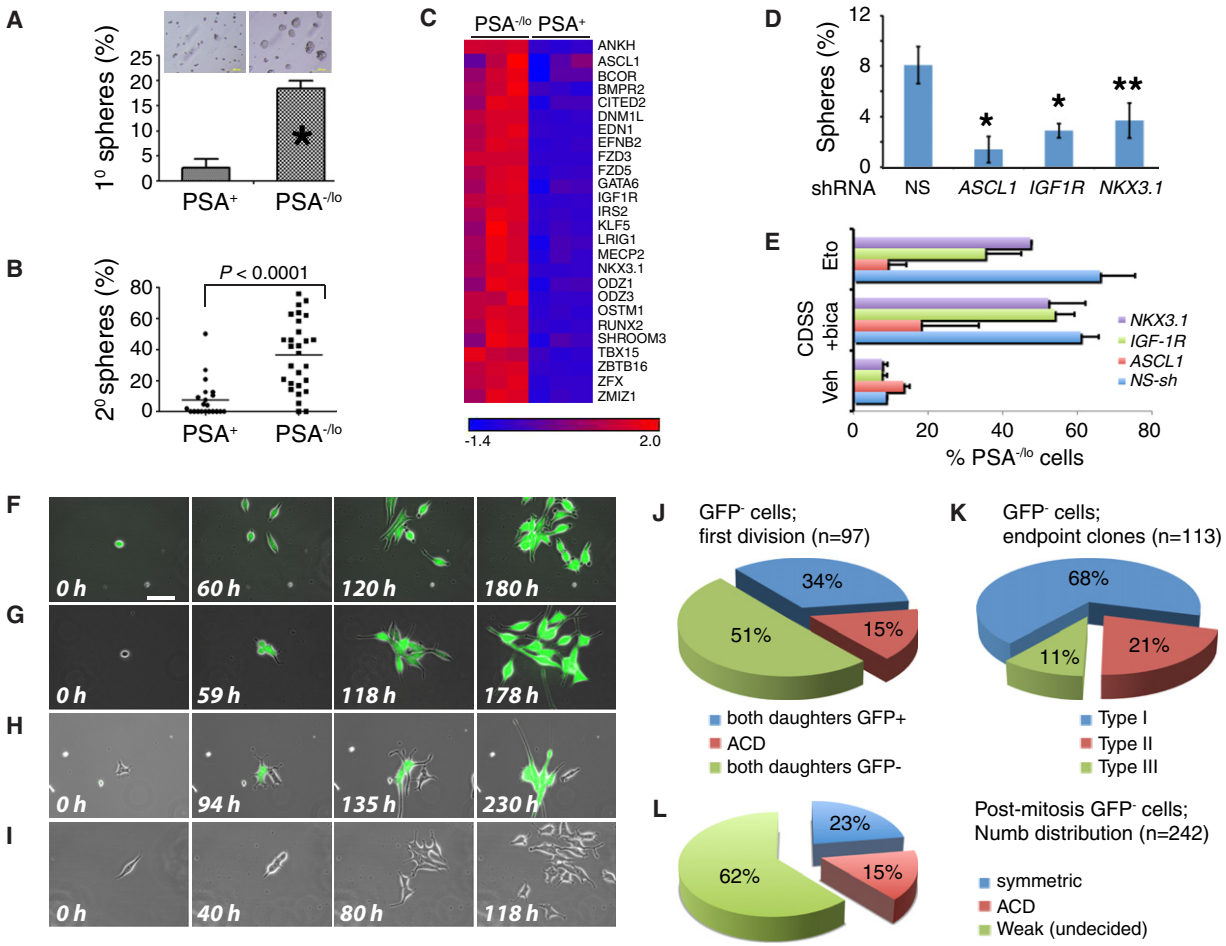

Figure 2. Distinct Biological Properties and Division Mode of PSA$^{-/lo}$ LNCaP Cells

(A) PSA$^{-/lo}$ LNCaP cells possess high sphere-forming capacity. Shown is the sphere-forming efficiency (%; *p < 0.0001) 10 days after plating. Insets show spheres generated from PSA^{+} (left) and PSA$^{-/lo}$ cells.

(B) PSA$^{-/lo}$ LNCaP cells possess higher 2° sphere-forming capacity than PSA^{+} cells. Individual 1° spheres in (A) were picked, dissociated, and used in 2° sphere assays.

(C) Heat map presentation of some SC-associated genes overexpressed in PSA$^{-/lo}$ LNCaP cells.

(D) Knocking down of *ASCL1*, *IGF-1R*, or *NKX3.1* in PSA$^{-/lo}$ LNCaP cells reduced sphere formation. Bars represent mean ± SD (n = 3).

(E) Knocking down of *ASCL1*, *IGF-1R*, or *NKX3.1* inhibited expansion of PSA$^{-/lo}$ (i.e., GFP^{-}) cells. LNCaP cells that had been stably knocked down for the three genes were infected with PSAP-GFP and then treated with DMSO (vehicle), CDSS plus bicalutamide (20 μM), or etoposide (Eto., 50 μM) for 7 days. Bars represent mean ± SD (n = 3).

(F–I) Single PSA^{+} (F) and PSA$^{-/lo}$ (G–I) LNCaP cells were tracked under a time-lapse video microscope. Images in (F) show symmetric cell division from a GFP^{+} LNCaP cell (representative of 52 movies; see Movie S1 for an example), and images in (G)–(I) represent type I, type II, and type III clones, respectively, derived from single GFP^{-} cells (from 292 movies; see Movie S1 for examples). Scale bar represents 20 μm.

(J) Quantification of cell division mode in GFP^{-} cells during the first cell division (n = 97 movies).

(K) Quantification of the type of clones derived from GFP^{-} cells at the end of recording (n = 113 movies).

(L) Asymmetric Numb segregation during divisions of GFP^{-} LNCaP cells in the single thymidine block and postmitosis Numb staining experiment.

enriched in stem cells (SCs) (Laffin and Tang, 2010). In support of this, the PSA$^{-/lo}$ LNCaP cells, in androgen/serum-free medium, possessed higher capacity to establish holoclones (Figure S3E) and anchorage-independent prostaspheres (Figure 2A). The PSA$^{-/lo}$ cell-derived spheres were much larger (Figure 2A, insets) and generated significantly more secondary spheres than the PSA^{+} cell-originated spheres (Figure 2B). PSA$^{-/lo}$ LNCaP cells also preferentially expressed many SC and developmental genes, such as ASCL1, CTED2, GATA6, IGF-1R, KLF5, LRIG1, NKX3.1, and TBX15 (Figure 1H; Figure 2C; Table S2). We employed tetracycline-inducible pTRIPZ lentiviral shRNAmir system to knock down three representative SC molecules, i.e., ASCL1 (Jiang et al., 2009), NKX3.1 (Wang et al., 2009b), and IGF-1R (Chan et al., 1998) (Figure S3I) in PSA$^{-/lo}$ LNCaP cells. Knocking down each of these molecules reduced sphere formation of PSA$^{-/lo}$ LNCaP cells (Figure 2D) without affecting the inherently low sphere-forming activity in PSA^{+} LNCaP cells (data not shown). Furthermore, ASCL1 knockdown significantly inhibited ($p < 0.05$), whereas IGF-1R or NKX3.1 knockdown partially reduced, the expansion of PSA$^{-/lo}$ cells caused by

androgen deprivation and etoposide (Figure 2E). These results suggest that at least some of the "stemness" genes overexpressed in the PSA$^{-/lo}$ LNCaP cells are functionally important.

Interestingly, PSA$^{-/lo}$ LNCaP cells, compared to PSA^{+} cells, overexpressed some (e.g., EED, HDAC4, PHF8) but underexpressed other (e.g., DNMT3B, PHF19) chromatin modifiers/epigenetic regulators (Figure S3J; Table S2). The functional significance of these changes in regulating the epigenetic landscape of PSA$^{-/lo}$ PCa cells is currently explored by genome-wide ChIP-Seq analysis.

PSA$^{-/lo}$ LNCaP Cells Can Undergo Asymmetric Cell Division and Regenerate PSA^{+} Cells

LNCaP cultures in RPMI-7% FBS contained ~1.4% of GFP$^{-/lo}$ cells, with the bulk being GFP^{+} (Figure S4A). When purified cells were cultured continuously for ~3 weeks, GFP^{+} LNCaP cells remained all GFP^{+} (Figure S4B), whereas GFP^{-} cultures became heterogeneous, containing 1.8% GFP^{-} cells and ~75% GFP-bright cells (Figure S4C). The 2° GFP^{+} LNCaP cultures derived from 1° GFP^{-} cells continued to remain all GFP^{+} after an additional 17-day culture (Figure S4D), whereas the 2° GFP^{-} cultures continued to regenerate both GFP^{-} and GFP^{+} cells (data not shown). Clonal development assays (Patrawala et al., 2005, 2006) revealed that cells in the clones derived from single GFP^{+} LNCaP cells remained 100% GFP^{+} at 2 (Figure S4E) and 4 (data not shown) weeks. In contrast, single GFP$^{-/lo}$ LNCaP cells developed into three distinct types of clones: type I with all cells being GFP^{+}, type II containing both GFP^{+} and GFP$^{-/lo}$ cells, and type III containing all GFP$^{-/lo}$ cells (Figures S4F–S4H). Quantitative analysis demonstrated that by 2 weeks, 70%–80% of all clones derived from single GFP$^{-/lo}$ LNCaP cells were type I and ~20% were type II, whereas the rest were type III (Figures S4I and S4J). Type I clones were likely derived from the cells that, at the sorting, had already committed to differentiation. Type III clones might all be PSA$^{-/lo}$ cells that underwent symmetric self-renewal based on PCR exclusion of noninfection (Figure 1C). Regardless, the emergence of type II clones indicated that ~20% PSA$^{-/lo}$ LNCaP cells were able to undergo asymmetric cell division (ACD), regenerating PSA$^{-/lo}$ and giving rise to PSA^{+} cells.

Because ACD is the cardinal feature of SCs (Knoblich, 2008), we used time-lapse videomicroscopy to further study the clonal development of PSA^{+} versus PSA$^{-/lo}$ LNCaP cells. In agreement with our "static" clonal analysis (above), live imaging of single GFP^{+} cells showed that the PSA^{+} LNCaP cells only underwent symmetric division, generating clones that contained all PSA^{+} cells (Figure 2F; Movie S1). By contrast, single GFP^{-} cells generated type I (Figure 2G; Movie S1), type II (Figure 2H; Movie S1), and type III (Figure 2I; Movie S1) clones. Approximately 15% of the GFP^{-} LNCaP cells underwent ACD during the first cell division, with one daughter cell becoming GFP^{+} (Figure 2J). Analysis of the end-point clones derived from single GFP^{-} cells showed that 21% and 11% clones were of type II and type III, respectively (Figure 2K).

To further explore asymmetric PCa cell division, we examined Numb partition during or right after mitosis. Numb is a Notch antagonist preferentially segregated into the differentiated daughter cells during asymmetric divisions of neuronal, hematopoietic, and muscle SCs (Knoblich, 2008; Wu et al., 2007). We observed that in 242 GFP^{-} LNCaP cells that had just undergone mitosis, 15% of the cells preferentially segregated Numb to the daughter cell that also expressed more PSA (Figure 2L; Figure 3A). In such cells, Numb showed typical cortical concentration (Figure 3A), consistent with its well-established roles in cell polarity and ACD. Using "mitotic shake-off" strategy, we observed similar asymmetric cosegregation of PSA and Numb in one daughter cell in some GFP^{-} LNCaP cells (Figure 3B, a–d), whereas in LNCaP cells that underwent symmetric division, Numb was also equally distributed in both cells (Figure 3B, e–h). Finally, we coinfected LNCaP cells with PSAP-GFP and a Numb-DsRed fusion retroviral reporter. The DsRed^{+}/GFP^{-} LNCaP underwent ACD at 6 hr, when Numb was partitioned in only one daughter cell, and from 24 hr, the Numb^{+} daughter cell also started to express GFP (i.e., PSA; Figure 3C). These observations indicate that a subset of PSA$^{-/lo}$ LNCaP cells can undergo authentic ACD associated with Numb cosegregation into the differentiated PSA^{+} daughter cells.

PSA$^{-/lo}$ PCa Cells Purified from Xenografts Possess Long-Term Clonogenicity, Are Quiescent, and Can Undergo ACD

We used PSAP-GFP or the modified lentivectors to establish LAPC9 (and LAPC4) "reporter" tumors (Figure S5A). The LAPC4 and LAPC9 xenograft models contain both differentiated and undifferentiated PCa cells and, as such, are very useful in elucidating the cellular heterogeneity of PCa (Patrawala et al., 2005, 2006, 2007). Immunostaining using LAPC4 and LAPC9 cells purified from the reporter tumors revealed that most GFP^{+} cells stained strongly for PSA, whereas GFP$^{-/lo}$ tumor cells were generally negative or weak for PSA (Figures S5B and S5C). Western blotting (Figure 3D) and qPCR (data not shown) also revealed lower protein and mRNA levels of PSA and AR in GFP$^{-/lo}$ LAPC9 cells.

In serum-containing medium, PSA$^{-/lo}$ LAPC9 cells initiated spheres that gradually enlarged and expanded and could be passaged for at least four generations, whereas PSA^{+} cell-initiated spheres aborted by 2° generation, despite that they formed slightly more 1° spheres (Figure 3E; Figure S5D), suggesting that PSA$^{-/lo}$ LAPC9 cells possess high sphere-propagating capacity. When PSA^{+} and PSA$^{-/lo}$ LAPC9 cells were cultured in medium containing CDSS, PSA$^{-/lo}$ cells formed much more (Figure 3F) and larger (Figure S5E) spheres than PSA^{+} cells. Interestingly, purified PSA$^{-/lo}$ LAPC4 cells founded more and larger spheres in both serum- (Figure S5F, a–c) and bicalutamide-containing (Figure S5F, d–f) media. Similar to PSA$^{-/lo}$ LNCaP cells, the PSA$^{-/lo}$ LAPC9 cells in the tumors were quiescent, as assessed by in vivo BrdU LRC (Figure 3G) and PKH26 dye-retaining (Pece et al., 2010) (Figure S6A) assays. Finally, we infected LAPC9 cells with PSAP-GFP/Pcmv-DsRed (Figure S3A), plated the purified PSA$^{-/lo}$ (i.e., DsRed^{+}/GFP^{-}) cells on fibroblast feeder, and tracked their developmental fates. Although most PSA$^{-/lo}$ LAPC9 cells underwent symmetric cell division (Figure 3H, top), ~5% cells underwent ACD, generating PSA^{+} LAPC9 cells (i.e., DsRed^{+}/GFP^{+}, yellow; Figure 3H, bottom).

PSA$^{-/lo}$ LAPC9 Cells Express Genes Associated with SC Functions and Castration Resistance

Microarray profiling revealed that ~200 genes were overexpressed, whereas ~300 genes were underexpressed (FC $\geq$ 1.4,

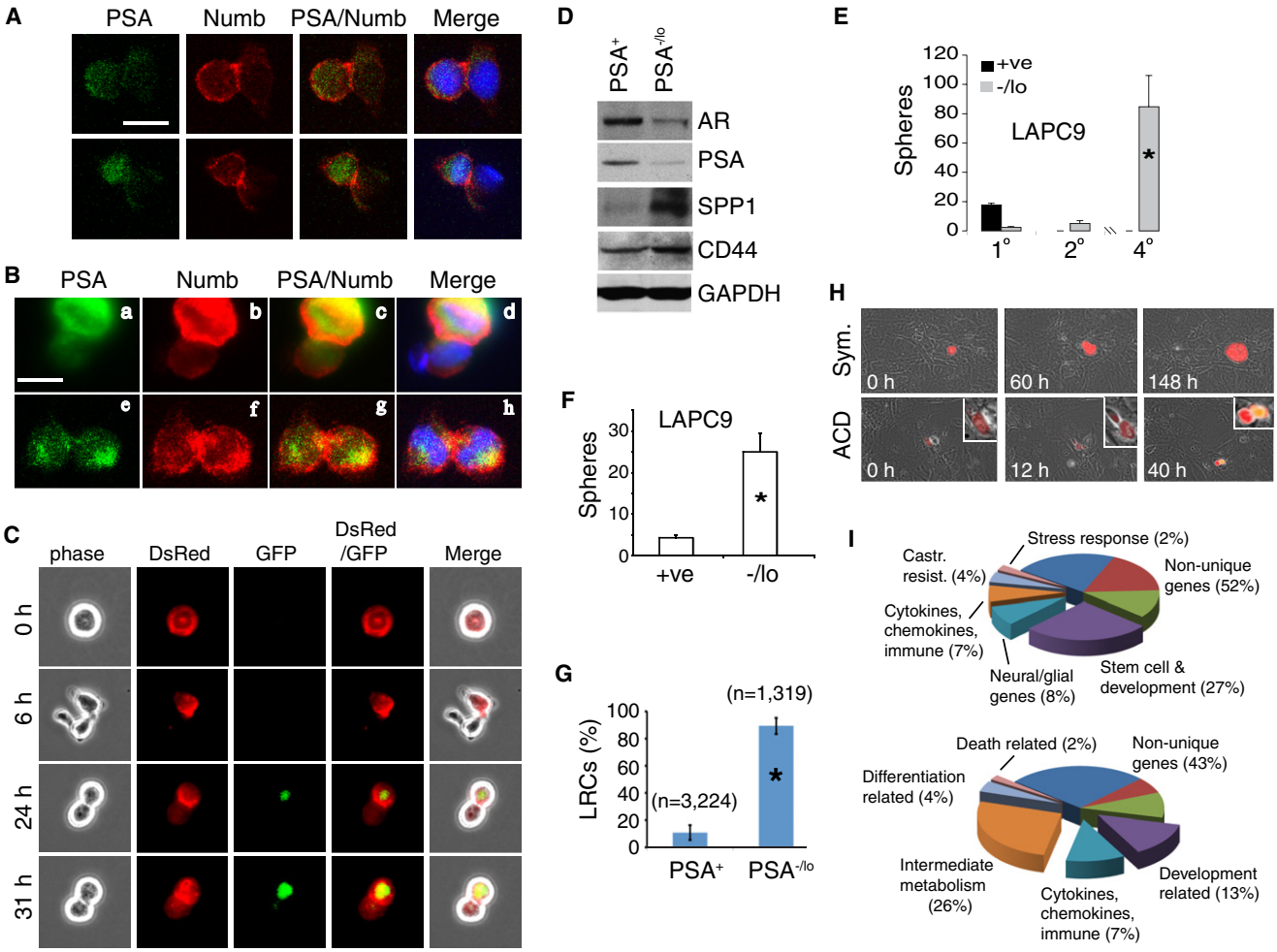

Figure 3. Distinct Biological Properties of PSA$^{-/lo}$ LNCaP and LAPC9 Cells

(A) Two representative GFP$^-$ LNCaP cells cosegregating PSA and Numb into one daughter cell during the first cell division (scale bar represents 20 μm).

(B) Different distribution patterns of PSA and Numb during asymmetric (Ba–Bd) and symmetric (Be–Bh) division of LNCaP cells assessed in the mitotic shake-off experiments. Images shown are representative of about five dozens of cells for each mode of cell division (scale bar represents 20 μm).

(C) Asymmetric cosegregation of Numb and PSA during ACD of PSA$^{-/lo}$ LNCaP cells assessed by time-lapse videomicroscopy. Shown are images of a PSA$^-$ (i.e., DsRed$^+$/GFP$^-$) LNCaP cell undergoing ACD by asymmetrically segregating Numb into one daughter cell, which subsequently acquired GFP (PSA) positivity (representative of a total of 188 similar movies analyzed).

(D) Western blotting analysis of the molecules indicated in purified PSA$^+$ and PSA$^{-/lo}$ LAPC9 cells.

(E and F) Purified PSA$^+$ and PSA$^{-/lo}$ LAPC9 cells were cultured (10,000 cells/well) in anchorage-independent conditions in either IMDM-15% FBS (E) or IMDM-15% CDSS (F) for 3 weeks, and spheres were enumerated. Shown in (E) is serial sphere passaging (see also Figure S5D). *$p < 0.01$.

(G) PSA$^{-/lo}$ LAPC9 cells were quiescent, as analyzed by in vivo LRC assays. *$p < 0.0001$.

(H) PSA$^{-/lo}$ (i.e., DsRed$^+$/GFP$^-$) LAPC9 cells undergo symmetric (top) or asymmetric (bottom) cell divisions assessed by time lapse. Images are representative of 65 movies analyzed.

(I) Distinct gene expression profiles of PSA$^{-/lo}$ and PSA$^+$ LAPC9 cells. Shown are pie charts of gene categories (percentage indicated) overexpressed (top) and underexpressed (bottom) in PSA$^{-/lo}$ cells.

$p < 0.05$) in PSA$^{-/lo}$ LAPC9 cells, which fall into distinct functional categories (Figure 3I; Table S3; Table S4). Most prominently, ~27% of genes (>50) overexpressed in PSA$^{-/lo}$ LAPC9 cells were associated with SCs and development, which included SPP1 (osteopontin or OPN), FGFs, ALDH1A1, integrin α2, c-KIT, Bcl-2, IGF-1, CD44, and Nanog (Figure 3I, top; Table S3; Table S4). Overexpression of some of these molecules was confirmed by western blotting (Figure 3D) and/or qPCR (Figure S6B). Many of the upregulated genes including Bcl-2, IGF-1, IGFBP3, REG4, and Nanog have been implicated in resistance to androgen deprivation (Jeter et al., 2011). Intriguingly, the PSA$^{-/lo}$ LAPC9 cells overexpressed about 20 neural/glial-related genes (Table S4), suggesting that PSA$^{-/lo}$ cells might be related to or have the ability to generate neuroendocrine-like cells. Finally, many genes preferentially expressed in PSA$^{-/lo}$ LAPC9 cells were shared with those expressed in ESCs or with the genes having either bivalent or H3K27me3 chromatin marks (Figure S6C). The major class of genes upregulated in PSA$^+$ LAPC9

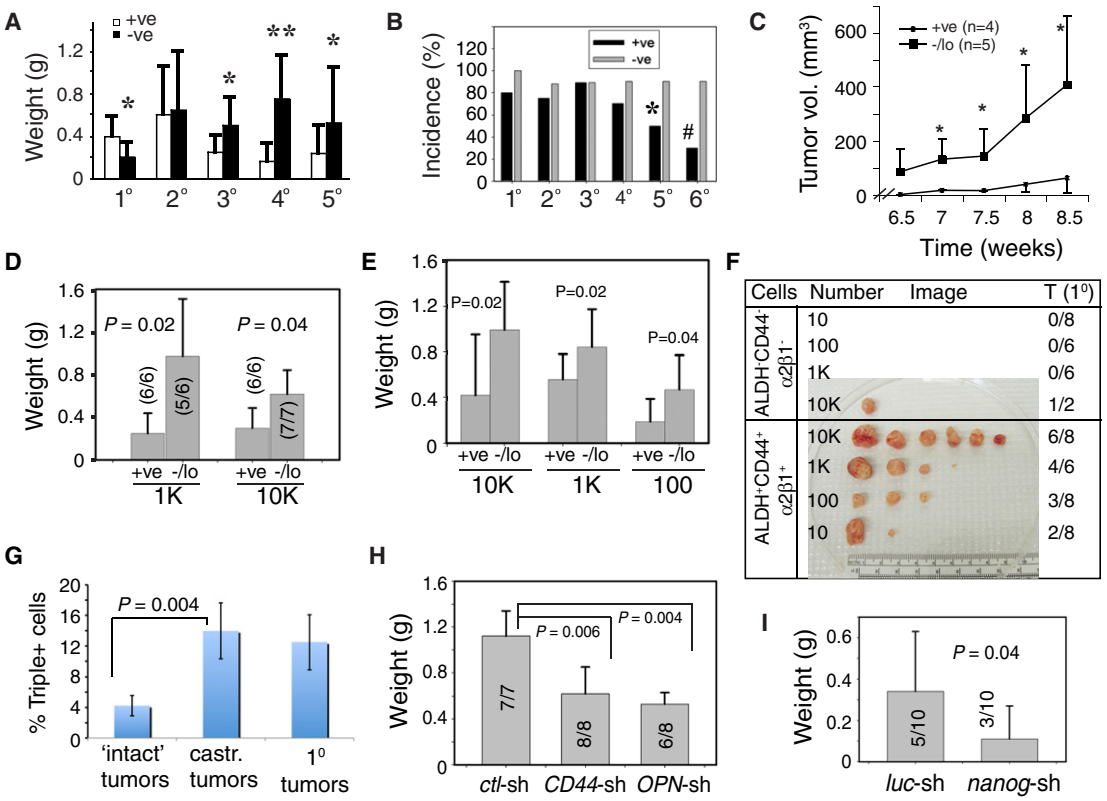

Figure 4. PSA$^{-/lo}$ PCa Cells Possess High and Long-Term Tumor Propagating Capacity

(A and B) Tumor weights (A; mean ± S.D, *p < 0.05, **p < 0.01) and incidence (B; *p = 0.045, #p = 0.006) of PSA$^+$ (+ve) and PSA$^{-/lo}$ (−/lo) LAPC9 cells serially transplanted in male NOD/SCID mice (see also Figure S7A).

(C and D) GFP$^+$ (+ve) and GFP$^-$ (−/lo) LAPC9 cells were acutely purified out and implanted subcutaneously in castrated male NOD/SCID mice treated with bicalutamide. (C) Tumor volumes measured in animals with 1,000 cell injections starting from 6.5 weeks postimplantation (mean ± SD; *p < 0.05; tumors harvested at 66 days for 1,000 cells and 60 days for 10,000 cells). Shown in (D) are incidence and weight.

(E) Purified GFP$^+$ (+ve) and GFP$^-$ (−ve) LAPC9 cells were implanted subcutaneously in female NOD/SCID mice. Tumors were harvested at 78 days (for 100 cells), 66 days (for 1,000 cells) or 53 days (for 10,000 cells) postimplantation.

(F) Triple marker-positive and -negative LAPC9 cells were purified from AI tumors and reimplanted, at the cell doses indicated, in fully castrated NOD/SCID mice.

(G) The percentage of triple marker-positive LAPC9 cells in three types of tumors, i.e., "intact" tumors maintained in hormonally intact male mice, "castrated" tumors maintained in castrated animals, and the 1° tumors derived from the triple marker-positive cells.

(H) Knockdown of OPN or CD44 inhibits tumor regeneration in PSA$^{-/lo}$ LAPC9 cells. PSA$^{-/lo}$ LAPC9 cells infected with control shRNA (ctl-sh), or CD44 or OPN shRNAs were implanted subcutaneously in male NOD/SCID mice. Bars represent tumor weights (mean ± SD).

(I) Nanog knockdown inhibits tumor regeneration. Shown are tumor weights and incidence. luc-sh, luciferase-shRNA; nanog-sh, Nanog-shRNA.

cells (26%) was involved in intermediated metabolism and, interestingly, NumbL, the mammalian homolog of Numb, was overexpressed in PSA$^+$ cells (Figure 3I, bottom; Table S3).

PSA$^{-/lo}$ PCa Cells Possess Long-Term Tumor-Propagating Capacity in Hormonally Intact Male Mice

Next, we performed limiting-dilution assays (LDAs) and serial tumor transplantation assays by monitoring tumor latency, incidence, growth rate, and/or endpoint weight. We first implanted 10,000 each of PSA$^{-/lo}$ (i.e., GFP$^{-/lo}$) and PSA$^+$ (GFP$^+$) LAPC9 cells subcutaneously in hormonally intact male NOD/SCID mice. Surprisingly, PSA$^+$ LAPC9 cells readily regenerated primary (1°) tumors that were about twice as large as those derived from PSA$^{-/lo}$ cells (Figure 4A; Figure S7A). When we infected LAPC9 cells with PSAP-GFP/Pcmv-DsRed and purified out PSA$^+$ (GFP$^+$DsRed$^+$) and PSA$^{-/lo}$ (GFP$^-$DsRed$^+$) cells for LDAs, the former demonstrated higher tumor-regenerating capacity (Table 1) and developed larger tumors (data not shown). Similarly, when PSA$^+$ and PSA$^{-/lo}$ LAPC9 cells were implanted orthotopically in the dorsal prostate (DP), PSA$^+$ cells initiated more (Table 1) and larger (data not shown) tumors. The PSA$^+$ LNCaP cells implanted in testosterone-supplemented male NOD/SCID mice also initiated larger tumors (Table 1). These findings suggest that "differentiated" PSA$^+$ PCa cells are, unexpectedly, tumorigenic in androgen-proficient hosts.

Nevertheless, when PSA$^+$ and PSA$^{-/lo}$ LAPC9 cell-derived tumors were serially passaged in intact male mice, PSA$^{-/lo}$ cells maintained relatively constant tumorigenicity, whereas PSA$^+$ cells displayed decreasing tumorigenicity (Figures 4A and 4B; Figure S7A). By 2° generation, tumor weights between the two groups became almost equal, and starting from the 3° generation, PSA$^+$ cells generated tumors two to three times smaller than PSA$^{-/lo}$ cell-derived tumors (Figure 4B; Figure S7A). Tumor growth rates also showed contrasting patterns: although the

Table 1. Tumor-Initiating Frequency of PSA$^+$ and PSA$^{-/lo}$ PCa Cells in NOD/SCID Mice

Cells	Cell Dose 10^5	10^4	10^3	10^2	10	1	Tumor-Initiating Frequency (95% Interval)[a]	p Value[a]
LNCaP								
PSA$^+$ (male)		2/4 (1.0 g)						
PSA$^{-/lo}$ (male)		3/5 (0.3 g)						
PSA$^+$ (castr.)		0/6						
PSA$^{-/lo}$ (castr.)		2/6 (1.3 g)						
PSA$^+$ (female)		1/6 (0.5 g)	1/6 (0.05 g)				1/30,110 (1/7,199–125,944)	
PSA$^{-/lo}$ (female)		4/5 (1.4 g)	5/7 (0.7 g)				1/2,674 (1/986–7,250)	0.0005
LAPC9								
PSA$^+$ (male)[b]		2/2	5/6	4/10	4/10	1/8	1/204 (1/88–473)	
PSA$^{-/lo}$ (male)[b]		1/2	4/6	4/10	2/10	0/8	1/552 (1/243–1,254)	0.0335
PSA$^+$ (male)/DP[c]	1/1	3/4	3/7				1/4,156 (1/1,518–11,382)	
PSA$^{-/lo}$ (male)/DP[c]	1/1	1/4	1/7				1/20,187 (1/5,125–79,523)	0.0399
PSA$^+$ (castr.)[b]			2/4	3/10	1/10	0/8	1/615 (1/238–1,589)	
PSA$^{-/lo}$ (castr.)[b]			2/4	2/10	2/9	1/8	1/196 (1/77–499)	0.075
PSA$^+$ (castr.)[c]		6/6	6/6				1/1 (1/1–1,071)	
PSA$^{-/lo}$ (castr.)[c]		7/7	5/6				1/559 (1/206–1,515)	0.224
PSA$^+$ (female)[c]		6/6	4/6	5/8			1/425 (1/180–1,006)	
PSA$^{-/lo}$ (female)[c]		6/8	5/6	6/8			1/235 (1/92–605)	0.254
ALDH^{hi}CD44$^+\alpha2\beta1^+$ (castr.) 1°[d]		6/8	4/6	3/8	2/8	0/8	1/448 (1/193–1,043)	
ALDH^{lo}CD44$^-\alpha2\beta1^-$ (castr.) 1°[d]		1/2	0/6	0/6	0/8	0/8	1/21,298 (1/3,126–145,130)	648×10^{150}
ALDH^{hi}CD44$^+\alpha2\beta1^+$ (castr.) 2°[d]			7/8	5/8	0/8	0/8	1/283 (1/125–645)	
ALDH^{lo}CD44$^-\alpha2\beta1^-$ (castr.) 2°[d]		2/3	0/8	0/8			1/13,802 (1/3,366–53,421)	2.23×10^9
LAPC4								
PSA$^+$ (male) 3°		6/10	4/8				1/6,895 (1/3,374–14,088)	
PSA$^{-/lo}$ (male) 3°		10/10	8/8				1/1 (1/1–860)	9.65×10^8

For LNCaP: PSA$^+$ (i.e., GFP$^+$) and PSA$^{-/lo}$ (GFP$^{-/lo}$) LNCaP cells were purified and implanted subcutaneously in 50% Matrigel in three types of NOD/SCID mice, i.e., intact male mice supplemented with testosterone pellets, surgically castrated (castr.) male mice also treated with bicalutamide, or female mice. All tumors were harvested 3–4.5 months after implantation.

For LAPC9: See footnotes.

For LAPC4: Shown are the tumor LDAs performed with the third-generation LAPC4 reporter tumors (see Figure S7B).

[a]Tumor-initiating frequency and statistical differences (p values) were determined using the Limdil function of the Statmod package (http://bioinf.wehi.edu.au/software/elda/index.html).

[b]LAPC9 cells acutely purified from xenograft tumors were infected with PSAP-GFP/Pcmv-DsRed (moi 20; 72 hr). Purified PSA$^+$ (i.e., GFP$^+$DsReD$^+$) and PSA$^{-/lo}$ (GFP$^-$DsRed$^+$) cells at the indicated numbers were injected subcutaneously into the intact or castrated male mice. All tumors were harvested in 2–3 months.

[c]PSA$^+$ (i.e., GFP$^+$) and PSA$^{-/lo}$ (i.e., GFP$^{-/lo}$) LAPC9 cells were purified out from reporter tumors. Cells at the indicated numbers were implanted subcutaneously or orthotopically (in the dorsal prostate) in 50% Matrigel in the three types of hosts. All tumors were harvested in ~2 months.

[d]The triple marker-positive and -negative LAPC9 cells were purified from the xenograft tumors that were maintained long-term in castrated NOD/SCID mice and injected at the indicated cell doses. Tumors were harvested ~2 months postimplantation. Then triple marker-positive and -negative cells were purified from the two tumors initially derived from ten marker-positive cell injections and used in secondary transplantations, which were harvested 73 days later.

1° PSA$^+$ LAPC9 tumors grew faster than PSA$^{-/lo}$ tumors, starting from the 3° generation, the PSA$^{-/lo}$ tumors grew much faster (data not shown). Importantly, although initially there was no significant difference in tumor incidence between the PSA$^+$ and PSA$^{-/lo}$ groups, by the 5° generation tumor incidence was lower for PSA$^+$ cells, and, by the 6° generation, tumor incidence was significantly lower ($p = 0.006$) for PSA$^+$ cells (Figure 4B; Figure S7A). Comparing tumor incidence across PSA$^+$ generations revealed that the 6° tumor incidence was much lower than that in the earlier (i.e., 1°–4°) generations ($p = 0.007$; proportion trend test). These observations indicate that PSA$^{-/lo}$ LAPC9 cells are endowed with long-term tumor-propagating capacity in androgen-proficient male hosts.

Similarly, the 1° PSA$^+$ LAPC4 tumors were slightly larger than those derived from PSA$^{-/lo}$ cells, but later-generation PSA$^+$ LAPC4 cells regenerated significantly smaller tumors than the corresponding PSA$^{-/lo}$ or early-generation PSA$^+$ cells (Figure S7B). Slightly different from LAPC9, PSA$^{-/lo}$ LAPC4 cells consistently demonstrated higher tumor incidence than PSA$^+$ cells across generations (Figure S7B; Table 1).

Consistent with the PSA$^{-/lo}$ LNCaP and LAPC9 cells being able to undergo ACD, generating both PSA$^{-/lo}$ and PSA$^+$ cells,

whereas PSA$^+$ cells undergo only symmetric divisions, most tumor cells in PSA$^+$ LNCaP cell-derived tumors in male mice were GFP$^+$/PSA$^+$, whereas tumors derived from PSA$^{-/lo}$ LNCaP cells contained both GFP$^+$/PSA$^+$ and GFP$^-$/PSA$^-$ cells (Figure S7C). Likewise, most tumor cells in PSA$^+$ LAPC9 cell-derived tumors serially passaged in male mice were GFP$^+$/PSA$^+$, whereas tumors derived from PSA$^{-/lo}$ cells contained both GFP$^+$/PSA$^+$ and GFP$^-$/PSA$^-$ cells (data not shown). FACS analysis demonstrated that tumors derived from GFP$^+$ LAPC9 cells contained mostly GFP$^+$ cells, whereas tumors derived from PSA$^{-/lo}$ LAPC9 cells contained ~20% GFP$^{-/lo}$ cells, with the majority of cells being GFP$^+$ (Figure S7D), indicating that the GFP$^{-/lo}$ PCa cells can undergo self-renewal and recreate the cellular heterogeneity in vivo.

PSA$^{-/lo}$ Cells Harbor CRPC-Regenerating Subpopulation that Can Be Further Enriched by the ALDH$^+$CD44$^+\alpha2\beta1^+$ Profile

We then implanted purified PSA$^+$ and PSA$^{-/lo}$ LAPC9 cells in castrated male NOD/SCID mice also treated with bicalutamide (50 mg/kg body weight; 3 times/week). In such "fully castrated" mice, PSA$^{-/lo}$ LAPC9 cells developed much larger tumors that grew significantly faster than corresponding PSA$^+$ cells (Figures 4C and 4D). In female NOD/SCID mice, often used as surrogate androgen-deficient hosts (Klein et al., 1997), PSA$^{-/lo}$ LAPC9 cells similarly initiated larger tumors than PSA$^+$ cells (Figure 4E). Purified PSA$^{-/lo}$ LNCaP cells also regenerated larger and/or more tumors in fully castrated male or female NOD/SCID mice (Table 1). These results suggest that the PSA$^{-/lo}$ PCa cells are more tumorigenic than PSA$^+$ cells in androgen-deficient hosts.

Intriguingly, the PSA$^{-/lo}$ LAPC9 cells did not display significantly higher tumor-initiating frequency, whether we utilized PSAP-GFP or PSAP-GFP/Pcmv-DsRed lentivectors to purify PSA$^+$ and PSA$^{-/lo}$ cells (Table 1). We reasoned that the PSA$^{-/lo}$ cell population was still heterogeneous, with tumorigenic cells that are able to initiate CRPC likely representing a minority. cDNA microarray analysis revealed the overexpression of ALDH1A1, integrin $\alpha2$, and CD44 in PSA$^{-/lo}$ LAPC9 cells (Table S3). ALDH1A1 is the major mediator of Aldefluor phenotype, and Aldefluor-hi (i.e., ALDH$^+$) population is enriched in cancer SCs (CSCs) (van den Hoogen et al., 2010), whereas CD44$^+$ PCa cells contain tumor-initiating cells (Patrawala et al., 2006) that can be further enriched by CD44$^+\alpha2\beta^+$ phenotype (Patrawala et al., 2007). Consequently, we purified ALDH$^+$CD44$^+\alpha2\beta1^+$ and ALDH$^-$CD44$^-\alpha2\beta1^-$ LAPC9 cells (Figure S7E) from the xenograft tumors maintained in castrated male NOD/SCID mice in which ~90% tumor cells were PSA$^{-/lo}$ and performed serial LDAs in fully castrated mice. Remarkably, ALDH$^+$CD44$^+\alpha2\beta1^+$ cells, in a cell dose-dependent manner, initiated tumor regeneration with as few as ten cells (Figure 4F; Table 1). In contrast, ALDH$^-$CD44$^-\alpha2\beta1^-$ cells only regenerated one tumor (out of 22 injections) at the highest cell number (Figure 4F), which likely resulted from cell impurity. Similar differences in tumorigenicity were observed between the two populations in the 2° transplantations (Table 1). The abundance of ALDH$^+$CD44$^+\alpha2\beta1^+$ cells was higher in castrate tumors than tumors in intact male mice and was maintained during serial transplantations (Figure 4G; data not shown), indicating the self-renewal of these cells in vivo. Combined, these results suggest that the ALDH$^+$CD44$^+\alpha2\beta1^+$ phenotype in PSA$^{-/lo}$ population further enriches CRPC cells.

To determine what molecules might be involved in determining the tumorigenicity of PSA$^{-/lo}$ PCa cells, we again resorted to our microarray data, which identified increased expression of Nanog, CD44, and OPN, among many others. Overexpression of Nanog, CD44, and OPN was confirmed by qPCR in independently purified PSA$^{-/lo}$ LAPC9 and other PCa cells (Figure S6B; data not shown). We therefore infected PSA$^{-/lo}$ LAPC9 cells with lentivectors encoding small hairpin RNA (shRNA) for Nanog (Jeter et al., 2009), OPN, or CD44 (Liu et al., 2011). Knockdown of OPN, CD44, or Nanog (Figures 4H and 4I) inhibited tumor regeneration of PSA$^{-/lo}$ LAPC9 cells in fully castrated hosts, consistent with our recent findings that CD44 knockdown inhibits PCa metastasis (Liu et al., 2011) and that Nanog overexpression promotes CSC properties and PCa cell resistance to androgen deprivation (Jeter et al., 2011).

PSA$^{-/lo}$ PCa Cells Resist Androgen Deprivation In Vivo

We carried out an ADT experiment (Yoshida et al., 2005) to determine whether PSA$^{-/lo}$ PCa cell-derived tumors resist androgen ablation in vivo. We purified PSA$^+$ and PSA$^{-/lo}$ LAPC9 cells and injected them into intact male mice. When tumors became palpable, mice were castrated and also treated with bicalutamide. PSA$^{-/lo}$ cell-derived tumors grew much better (Figure 5A) and larger (Figure 5B) in androgen-depleted hosts than PSA$^+$ cell-derived tumors. We further attempted to mimic the clinical scenario by correlating % GFP$^+$ (PSA$^+$) cells during castration with biochemical (PSA) failure and tumor recurrence (regrowth). When the group of animals bearing LAPC9 tumors was castrated and concomitantly treated with bicalutamide at week 5, tumor growth plateaued, serum PSA levels dipped, and the % GFP$^+$ cells declined by week 6 (Figure 5C). However, by week 8, despite continued decrease in GFP$^+$ cells (Figure 5C, right), tumor growth resumed (Figure 5C, left, inset) and serum PSA rebounded (Figure 5C, middle, inset), signaling biochemical recurrence (BCR) and tumor recurrence. These observations were remarkably similar to what was observed in PCa patients undergoing ADT (Ryan et al., 2006) and provide evidence that androgen ablation enriches PSA$^{-/lo}$ PCa cells.

The PSA$^{-/lo}$ Cells from Primary Prostate Tumors and Early Xenografts Were Also More Clonogenic and Tumorigenic

Are the preceding findings in PCa models (LNCaP, LAPC9, and LAPC4) applicable to patient tumors? Strikingly, low levels of tumor *PSA* mRNA correlated with reduced BCR-free and overall patient survival (Figure 6A). We purified primary prostate tumor (HPCa) cells from (untreated) prostatectomy specimens, infected them with PSAP-GFP, separated PSA$^+$ and PSA$^{-/lo}$ cells, and performed clonal and sphere assays in serum/androgen-free medium (Jeter et al., 2009; Liu et al., 2011). The results from three HPCa samples showed that PSA$^{-/lo}$ cells did not express AR protein (data not shown) and possessed significantly higher clonal and sphere-forming capacities than corresponding PSA$^+$ cells (Figures 6B–6D; Figure S8A). Importantly, we observed clonal development patterns in HPCa cells similar to those observed in LNCaP cells. For instance, most PSA$^+$ HPCa12 cell-derived clones were GFP$^+$, whereas the PSA$^{-/lo}$

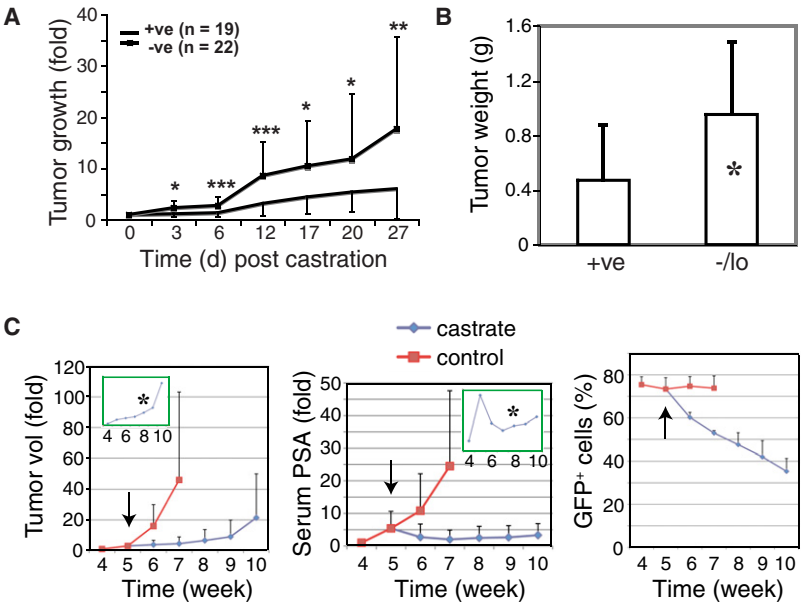

Figure 5. PSA$^{-/lo}$ PCa Cells Are More Resistant to Experimental ADT

(A and B) Purified PSA^{+}/PSA$^{-/lo}$ LAPC9 cells (10,000 each) were injected subcutaneously in intact male mice, and when tumors became palpable, mice were castrated and treated with bicalutamide (time 0). Tumors were measured at the indicated time points, and results are presented as fold increase in tumor growth over time 0 (F; *$p < 0.05$; **$p < 0.01$; ***$p < 0.001$). Shown in (B) are tumor weights (mean ± SD; *$p < 0.05$) from one group of animals at the end of experiments (see Table 1 for incidence).

(C) "Recurrence" experiments. Shown are measurements of tumor volume (left), serum PSA (middle), and the percentage of GFP^{+} LAPC9 cells in the tumors (right) starting from the fourth week after implantation. Arrows indicate the time of castration (i.e., the fifth week). Insets: tumor volume (left) and PSA (middle) plotted for the castrate group only (asterisks indicate when tumors "recurred" at 8 weeks).

cell-derived holoclones contained GFP$^{-/lo}$, as well as GFP^{+} cells (Figure 6E). Similar type II clones were observed in PSA$^{-/lo}$ cells plated on collagen (Figure 6F), and some PSA$^{-/lo}$ HPCa cells also underwent ACD (Figure 6G). Microarray analysis in four pairs of purified PSA$^{-/lo}$ and PSA^{+} HPCa cells revealed preferential expression of many SC/developmental genes in PSA$^{-/lo}$ HPCa cells (Table S5).

Using one of the early-generation (4°) HPCa xenografts, i.e., HPCa58 (Liu et al., 2011), we established reporter tumors similar to LAPC9 and LAPC4. The reporter tumor was green (Figure 6H) and expressed *PSA* mRNA (Figure 6I). PSA immunostaining revealed a good correlation between GFP and PSA positivity (Figure 6J). When PSA^{+} and PSA$^{-/lo}$ HPCa58 cells were used in sphere assays, the PSA$^{-/lo}$ cells demonstrated higher sphere-forming capacity in both androgen-supplemented (Figure S8B) and androgen-ablated (Figure S8C) conditions. Serial transplantations in male NOD/SCID mice revealed that PSA^{+} HPCa58 cells initiated larger tumors than the corresponding PSA$^{-/lo}$ cells in the first generation; however, upon passaging, PSA$^{-/lo}$ HPCa58 cells developed larger tumors than the corresponding PSA^{+} cells (Figure 6K). Finally, when equal numbers (10,000) of PSA^{+} and PSA$^{-/lo}$ HPCa58 cells were implanted in castrated male NOD/SCID mice treated with bicalutamide, PSA$^{-/lo}$ cells generated larger and more tumors (Figure S8D). Experiments with another HPCa reporter tumor, i.e., HPCa80, revealed that the PSA$^{-/lo}$ HPCa80 cells generated larger tumors than PSA^{+} HPCa80 cells (Figure S8E).

DISCUSSION

PSA$^{-/lo}$ PCa Cells, Tumor *PSA* mRNA, and Serum PSA: Relevance to PCa

PSA is normally expressed and secreted by prostate luminal cells and represents one of the best-characterized organ-specific differentiation markers. Early studies have shown that PSA protein expression in PCa positively correlates with its degree of differentiation and that both untreated PCa and CRPC contain PSA^{+} and PSA$^{-/lo}$ cancer cells. Our own analysis of ~45 patient tumors confirms the two populations of PCa cells and, importantly, demonstrates that the abundance of PSA$^{-/lo}$ PCa cells is enriched in high-grade and treatment-failed tumors. PSA protein is also reduced or lacking in metastases (Varambally et al., 2005). Strikingly, lower tumor *PSA* mRNA levels positively correlate with worse clinical outcomes, including high tumor grade, LN positivity, metastasis, recurrence, and reduced patient survival. The association of PSA$^{-/lo}$ PCa cells and tumor PSA mRNA/protein with poor clinical features is opposite to the positive correlation between serum PSA and the same clinical parameters. Elevated serum PSA levels in advanced PCa may be due to increased access of PCa cells to bloodstream and/or related to increased tumor mass in which PSA$^{-/lo}$ PCa cells can differentiate into PSA^{+} cells.

PSA$^{-/lo}$ PCa Cells and AR

PSA has been thought to be strictly regulated by AR. In clinical samples, however, AR and PSA protein expression is often discordant and heterogeneous, with some PCa cells showing little expression of either molecule (Hobisch et al., 1995; Mostaghel et al., 2007; Ruizeveld de Winter et al., 1994; Shah et al., 2004). Discordant AR and PSA expression is also reflected at the mRNA levels in individual primary, hormone-refractory, and recurrent tumors, as well as in metastases (Figure S2B; unpublished data). The discordant expression patterns of PSA and AR suggest that PSA expression can be regulated in an AR-independent manner (Hsieh et al., 1993) and that prostate tumors contain AR^{+}/PSA^{+}, AR^{+}/PSA^{-}, AR^{-}/PSA^{+}, and AR^{-}/PSA^{-} PCa cells.

The PSA^{+} PCa cells isolated based on our reporter systems mostly show strong nuclear AR, whereas PSA$^{-/lo}$ population contains both AR^{-} and AR^{+} cells. Consequently, PSA^{+} cells resemble AR^{+}/PSA^{+} cells, whereas PSA$^{-/lo}$ cells contain both AR^{+}/PSA^{-} and AR^{-}/PSA^{-} PCa cells. AR expression is sometimes upregulated in advanced and recurrent tumors, which we surmise could be related to the expansion of AR^{+}/PSA^{-} PCa cells. Future work that permits fractionation of AR^{+}/PSA^{-} and AR^{-}/PSA^{-} PCa

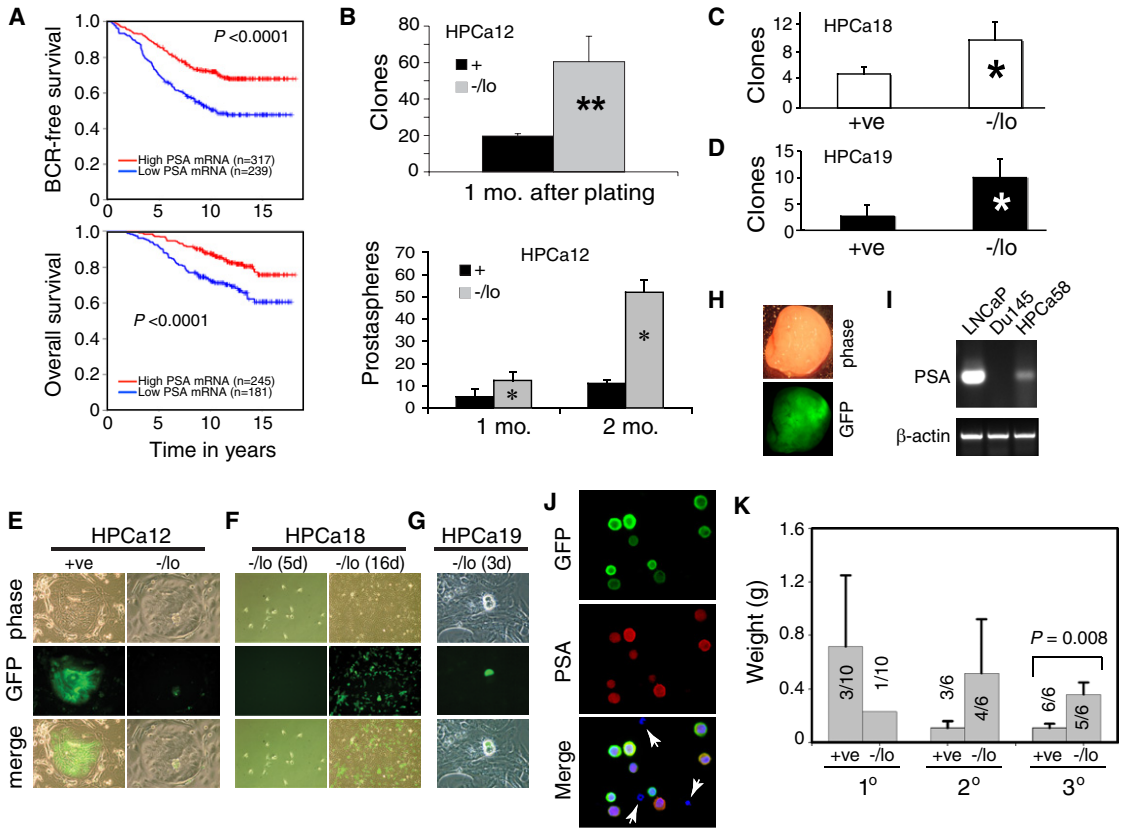

Figure 6. Distinct Biological and Tumor-Propagating Properties of PSA$^+$ and PSA$^{-/lo}$ HPCa Cells

(A) Meta-analysis showing lower tumor *PSA* mRNAs correlating with reduced BCR-free or overall patient survival. Data were based on the Nakagawa study (see Figure S2).

(B) PSA$^+$ and PSA$^{-/lo}$ HPCa12 cells were plated (2,000 cells/well) in serum/androgen-free PrEBM medium on Swiss 3T3 feeders for holoclone analysis (top; $^{**}p < 0.01$) or in low-attachment plate for sphere-formation assays (bottom; $^{*}p < 0.05$).

(C and D) PSA$^+$/PSA$^{-/lo}$ HPCa18 (C) and HPCa 19 (D) cells were plated (100 cells/well) and cultured on Swiss 3T3 feeder plate for 18 days, and individual holoclones were enumerated. $^{*}p < 0.05$.

(E–G) PSA$^+$ and PSA$^{-/lo}$ HPCa cells were purified from three patient tumors, infected, FACS purified, and plated (at 1 cell/well in 96 microwell plate) on either fibroblasts (E and G) or collagen (F). Images in E were taken 12 days postplating.

(H–K) Experiments with HPCa58 early xenograft tumors. HPCa58 cells were purified out from the 4° HPCa58 xenografts, infected with PSAP-GFP, and implanted subcutaneously in male NOD/SCID-γ mice to establish reporter tumors. (H) A representative reporter tumor. (I) RT-PCR of PSA mRNA. (J) PSA immunostaining in GFP$^+$ HPCa58 cells on cytospun slides (small white arrows, GFP$^-$ cells that were also PSA$^-$). (K) Tumor weights (mean ± SD) and incidence of serially transplanted PSA$^+$ (+ve) and PSA$^{-/lo}$ (−/lo) HPCa58 cells (10,000 cells/injection).

cells should allow us to directly address this postulate. It should be noted that AR possesses PCa-suppressive functions (Niu et al., 2008), AR signaling is attenuated in some advanced PCa (Tomlins et al., 2007), AR is significantly reduced and only detectable in ~40% PCa cells in hormone-refractory metastases (Davis et al., 2006), and AR requirement in PCa may be context dependent (Memarzadeh et al., 2011).

Distinct Biological Properties and Gene Expression Profiles of PSA$^{-/lo}$ PCa Cells

PSA$^{-/lo}$ PCa cells possess high clonogenic capacity, survive better in androgen-deficient conditions, and are refractory to not only androgen deprivation but also drugs. PSA$^{-/lo}$ PCa cells are quiescent, which could partly explain their resistance to various stresses. Importantly, a fraction of PSA$^{-/lo}$ PCa (~15%–20% PSA$^{-/lo}$ LNCaP and 5% PSA$^{-/lo}$ LAPC9) cells can undergo authentic ACD, a cardinal feature of SCs. In contrast, PSA$^+$ cells undergo mainly symmetric divisions. The distinct division patterns between PSA$^+$ and PSA$^{-/lo}$ cells overall are mirrored in the respective tumors they regenerate—although the PSA$^+$ cell-derived tumors contain mostly PSA$^+$ cells, the PSA$^{-/lo}$ cell-originated tumors contain both PSA$^{-/lo}$ and PSA$^+$ cells.

It is presently unclear how PSA$^{-/lo}$ and PSA$^+$ cells, both of which are maintained under identical conditions, embark on different developmental fates. Nevertheless, the distinct division modes of PSA$^{-/lo}$ and PSA$^+$ cells reinforce their intrinsic biological differences. Significantly, the PSA$^+$ differentiated daughter cell derived from asymmetric division of a PSA$^-$ PCa cell also preferentially "inherits" Numb, one of the best-studied cell fate determinants known to be asymmetrically segregated into differentiated daughter cells (Knoblich, 2008). It is interesting that asymmetric segregation of Numb precedes that of PSA (Figure 3J), raising the possibility that Notch signaling may regulate PCa cell ACD.

PSA$^{-/lo}$ LNCaP and LAPC9 cells preferentially express dozens of genes associated with development and SC functions. These SC-associated molecules are functionally important, as demonstrated for ASCL-1, IGF-1, and NKX3.1 in LNCaP cells and Nanog, CD44, and OPN in LAPC9 cells. The PSA$^{-/lo}$ LNCaP and LAPC9 cells commonly overexpress hundreds of genes (e.g., BCL2, IGF1, SOX15, BMPR1B, TGFBR1, etc.), which fall into distinct GO categories including SC, development, stress response, and wound healing (unpublished data).

The PSA$^{-/lo}$ LNCaP and LAPC9 cells do express "unique" gene categories. Thus, PSA$^{-/lo}$ LNCaP cells prominently underexpress genes associated with cell-cycle progression and mitosis. In contrast, the PSA$^{-/lo}$ LAPC9 cells overexpress hundreds of signaling molecules but underexpress genes associated with intermediate metabolism. The observations that PSA$^{-/lo}$ LNCaP cells underexpress cell-cycle and mitosis-associated genes and that PSA$^{-/lo}$ LAPC9 cells underexpress metabolism-associated genes are consistent with the PSA$^{-/lo}$ PCa cells being more quiescent. Intriguingly, PSA$^{-/lo}$ and PSA^{+} LAPC9 cells frequently exhibit reciprocal gene expression patterns (Table S4), suggesting that the two populations of PCa cells may crosstalk and reciprocally regulate each other in a "paracrine" fashion, as hinted by emerging data in other tumor systems (Tang, 2012).

Distinct Tumor-Propagating Properties of PSA$^{-/lo}$ Cells: Evidence for a Tumorigenic Pool that Harbors Distinct CSC Subsets

Tumor transplantation experiments in NOD/SCID mice (~2,000 used) reveal that, although the tumor-propagating capacities of PSA$^{-/lo}$ PCa cells are maintained across the generations in hormonally intact male mice, the tumor-regenerating ability of the corresponding PSA^{+} PCa cells gradually declines, suggesting that PSA$^{-/lo}$ cells possess long-term tumor-propagating capacity. The PSA$^{-/lo}$ cell-regenerated tumors recreate the original tumor heterogeneity containing both PSA$^{-/lo}$ and PSA^{+} cells. That PSA^{+} cells serially transplanted in androgen-proficient hosts manifest diminishing tumorigenic potential strongly suggests that these cells intrinsically possess more limited self-renewal ability compared to PSA$^{-/lo}$ PCa cells. The unexpected observations that PSA^{+} cells, at the first generation, often demonstrate higher tumorigenic potential than the isogenic PSA$^{-/lo}$ cells caution us to be careful when using tumor regeneration as a yardstick of measuring CSC properties. Preferably, serial transplantation assays should be performed; otherwise, misleading or even opposing/contradictory conclusions may be reached.

When transplanted in androgen-deficient hosts, PSA$^{-/lo}$ PCa cells initiate much larger and faster-growing tumors than isogenic PSA^{+} cells. Taken together, the biological, molecular, and tumorigenic properties of PSA$^{-/lo}$ cells presented herein, coupled with earlier reports on several prostate CSC populations (e.g., Collins et al., 2005; Huss et al., 2005; Maitland et al., 2011; Patrawala et al., 2006; Rajasekhar et al., 2011), suggest that the PSA$^{-/lo}$ cell population may represent a tumorigenic pool that harbors several subsets of stem-like cancer cells. First, CD133^{+} $\alpha2\beta1^{hi}$CD44^{+} primary PCa cells (Collins et al., 2005), ABCG2^{+} PCa cells in situ (Huss et al., 2005), and Lin^{-}CD44^{+} PCa cells in xenografts (Patrawala et al., 2006) all seem to express low levels of AR and to lack PSA, suggesting that these PCa cell subsets may overlap with each other and are all harbored in PSA$^{-/lo}$ population. Second, unbiased whole-genome transcriptome analysis reveals preferential expression of CD44, integrin $\alpha2$, and ALDH1A1 in PSA$^{-/lo}$ LAPC9 cells. Third, prospectively purified ALDH^{+}CD44$^{+}\alpha2\beta1^{+}$ subpopulation in PSA$^{-/lo}$ cells greatly enriches for more tumorigenic, castration-resistant PCa cells. Finally, CD44^{+} PCa cells freshly purified from a dozen untreated primary tumors express much lower levels of PSA mRNAs than the corresponding CD44^{-} PCa cells (X.L. et al., unpublished data). Future work will further elucidate the interrelationship between various subsets of tumorigenic cells and characterize PSA$^{-/lo}$ PCa cells with respect to their relationship with luminal and basal cells.

PSA$^{-/lo}$ CSCs May Represent an Important Source of CRPC Cells

One of the most significant contributions of the present work is to provide direct experimental evidence that PSA$^{-/lo}$ PCa cells may represent an important source of CRPC cells. First, PSA$^{-/lo}$ cells, in vitro, survive androgen deprivation, resist drug/stress treatments, and robustly found holoclones and self-renewing spheres. Second, when both PSA^{+} and PSA$^{-/lo}$ cells are implanted in male mice that are subsequently subjected to ADT, the PSA$^{-/lo}$ cell-derived tumors are refractory to castration and continue to develop. Third, androgen deprivation greatly enriches the PSA$^{-/lo}$ cells, which could initiate robust tumor development in castrated hosts. These findings closely resemble the AI progression observed in patients and mirror the observed reduction in PSA-producing cells in patient tumors upon androgen depletion (Ryan et al., 2006).

We have provided prospective evidence that PSA$^{-/lo}$ PCa cells, which preexist in the tumors, are molecularly and functionally distinct from the differentiated counterparts. We have shown that under normal (i.e., androgen-proficient) conditions, undifferentiated PSA$^{-/lo}$ cells harbor self-renewing CSCs and likely represent one important source of CRPC cells. Future work will address whether, under other conditions such as persistent castrations, PSA^{+} PCa cells may manifest increased plasticity by undergoing dedifferentiation, as shown by emerging data in other tumors (Tang, 2012). Altogether, our results suggest that novel therapeutics targeting PSA$^{-/lo}$ cells should be developed and used in conjunction with ADT in order to eradicate all PCa cells and prevent recurrence.

EXPERIMENTAL PROCEDURES

Detailed methods are available online in the Supplemental Experimental Procedures.

Serial Tumor Transplantation in NOD/SCID Mice

We sorted out GFP^{+} and GFP^{-} PCa cells by FACS from 1° tumors originally derived from GFP^{+} and GFP^{-} cells, respectively, and implanted subcutaneously to generate 2° tumors in intact male mice. We performed sequential tumor transplantation using similar strategies by following the procedure that GFP^{+} cells were always purified from tumors that originated from purified GFP^{+} cells, whereas GFP^{-} cells were from tumors derived initially from GFP^{-} cells. For tumor experiments in castrated mice, we surgically castrated male NOD/SCID mice (6–8 weeks) 1–2 weeks prior to injection. GFP^{+}/GFP^{-} PCa cells were purified out from reporter tumors and injected subcutaneously into the castrated mice, which also received intraperitoneal injections of bicalutamide.

Experimental ADT and "Recurrence" Experiments

For ADT, GFP$^+$ and GFP$^-$ LAPC9 cells were purified out from AD reporter tumors and injected subcutaneously in intact male NOD/SCID mice. When tumors reached ~60 mm^3, mice were surgically castrated and treated with bicalutamide. Tumor growth was followed by caliper measurement, and volumes of individual tumor were normalized to those on day 0 (day of castration). For "recurrence" experiments, unsorted LAPC9 cells from AD reporter tumors were injected subcutaneously in intact male NOD/SCID mice. Starting from the fourth week, tumor volumes (mm^3) were measured using a digital caliper, blood samples (100–200 μl/mouse) were collected from each animal via saphenous vein for serum PSA measurement (ng/ml), and two to three tumors were harvested to determine by FACS the percentage of GFP$^+$ cells in individual tumors on weekly basis. For tumor volumes and serum PSA, the values were presented as fold increases over those from the fourth week. At the fifth week, animals were randomly divided into the control group, in which the animals were mock castrated, and the castrate group, in which the animals were surgically castrated and also treated with bicalutamide.

Time-Lapse Videomicroscopy

Time-lapse fluorescence videomicroscopy was performed using Nikon Biostation Timelapse system (Liu et al., 2011), as described in the Supplemental Experimental Procedures.

cDNA Microarray

Basic procedures have been described (Bhatia et al., 2008). Total RNA was extracted from pooled purified GFP$^+$, GFP$^-$ LNCaP, LAPC9, or HPCa cells, and microarray experiments were performed in triplicates using the 44 K 60-mer Human Whole-Genome Oligo Microarray Kit from Agilent (Agilent Technologies, Santa Clara, CA) with 500 ng of total RNA. For details, please refer to the Supplemental Experimental Procedures.

SUPPLEMENTAL INFORMATION

Supplemental Information includes eight figures, five tables, Supplemental Experimental Procedures, and one movie and can be found with this article online at doi:10.1016/j.stem.2012.03.009.

ACKNOWLEDGMENTS

We thank K. Claypool and P. Whitney for FACS, Histology Core for immunohistochemistry, R. Fagin for HPCa samples, J. Shen and J. Repass for qPCR, L. Shen and S. Tsavachidis for initial microarray analysis, and other members of the Tang laboratory for helpful discussions. This work was supported in part by grants from the National Institutes of Health (R01-ES015888 and 1R21CA 150009), Department of Defense (W81XWH-11-1-0331), Cancer Prevention and Research Institute of Texas (RP120380 and RP120394), Elsa Pardee Foundation, and M.D. Anderson Cancer Center University Cancer Fund, Center for Cancer Epigenetics, and Laura & John Arnold Foundation RNA Center pilot grant (all to D.G.T.) and by two Center Grants (CCSG-5 P30 CA166672 and ES007784). We apologize to the colleagues whose work was not cited due to space constraint.

Received: August 10, 2011
Revised: January 25, 2012
Accepted: March 8, 2012
Published: May 3, 2012

REFERENCES

Abrahamsson, P.A., Lilja, H., Falkmer, S., and Wadström, L.B. (1988). Immunohistochemical distribution of the three predominant secretory proteins in the parenchyma of hyperplastic and neoplastic prostate glands. Prostate *12*, 39–46.

Bhatia, B., Jiang, M., Suraneni, M., Patrawala, L., Badeaux, M., Schneider-Broussard, R., Multani, A.S., Jeter, C.R., Calhoun-Davis, T., Hu, L., et al. (2008). Critical and distinct roles of p16 and telomerase in regulating the proliferative life span of normal human prostate epithelial progenitor cells. J. Biol. Chem. *283*, 27957–27972.

Chan, J.M., Stampfer, M.J., Giovannucci, E., Gann, P.H., Ma, J., Wilkinson, P., Hennekens, C.H., and Pollak, M. (1998). Plasma insulin-like growth factor-I and prostate cancer risk: a prospective study. Science *279*, 563–566.

Collins, A.T., Berry, P.A., Hyde, C., Stower, M.J., and Maitland, N.J. (2005). Prospective identification of tumorigenic prostate cancer stem cells. Cancer Res. *65*, 10946–10951.

Davis, J.N., Wojno, K.J., Daignault, S., Hofer, M.D., Kuefer, R., Rubin, M.A., and Day, M.L. (2006). Elevated E2F1 inhibits transcription of the androgen receptor in metastatic hormone-resistant prostate cancer. Cancer Res. *66*, 11897–11906.

Feiner, H.D., and Gonzalez, R. (1986). Carcinoma of the prostate with atypical immunohistological features. Clinical and histologic correlates. Am. J. Surg. Pathol. *10*, 765–770.

Gallee, M.P., Visser-de Jong, E., van der Korput, J.A., van der Kwast, T.H., ten Kate, F.J., Schroeder, F.H., and Trapman, J. (1990). Variation of prostate-specific antigen expression in different tumour growth patterns present in prostatectomy specimens. Urol. Res. *18*, 181–187.

Hobisch, A., Culig, Z., Radmayr, C., Bartsch, G., Klocker, H., and Hittmair, A. (1995). Distant metastases from prostatic carcinoma express androgen receptor protein. Cancer Res. *55*, 3068–3072.

Hsieh, J.T., Wu, H.C., Gleave, M.E., von Eschenbach, A.C., and Chung, L.W.K. (1993). Autocrine regulation of prostate-specific antigen gene expression in a human prostatic cancer (LNCaP) subline. Cancer Res. *53*, 2852–2857.

Huss, W.J., Gray, D.R., Greenberg, N.M., Mohler, J.L., and Smith, G.J. (2005). Breast cancer resistance protein-mediated efflux of androgen in putative benign and malignant prostate stem cells. Cancer Res. *65*, 6640–6650.

Jeter, C.R., Badeaux, M., Choy, G., Chandra, D., Patrawala, L., Liu, C., Calhoun-Davis, T., Zaehres, H., Daley, G.Q., and Tang, D.G. (2009). Functional evidence that the self-renewal gene NANOG regulates human tumor development. Stem Cells *27*, 993–1005.

Jeter, C.R., Liu, B., Liu, X., Chen, X., Liu, C., Calhoun-Davis, T., Repass, J., Zaehres, H., Shen, J.J., and Tang, D.G. (2011). NANOG promotes cancer stem cell characteristics and prostate cancer resistance to androgen deprivation. Oncogene *30*, 3833–3845.

Jiang, T., Collins, B.J., Jin, N., Watkins, D.N., Brock, M.V., Matsui, W., Nelkin, B.D., and Ball, D.W. (2009). Achaete-scute complex homologue 1 regulates tumor-initiating capacity in human small cell lung cancer. Cancer Res. *69*, 845–854.

Klein, K.A., Reiter, R.E., Redula, J., Moradi, H., Zhu, X.L., Brothman, A.R., Lamb, D.J., Marcelli, M., Belldegrun, A., Witte, O.N., and Sawyers, C.L. (1997). Progression of metastatic human prostate cancer to androgen independence in immunodeficient SCID mice. Nat. Med. *3*, 402–408.

Knoblich, J.A. (2008). Mechanisms of asymmetric stem cell division. Cell *132*, 583–597.

Laffin, B., and Tang, D.G. (2010). An old player on a new playground: bmi-1 as a regulator of prostate stem cells. Cell Stem Cell *7*, 639–640.

Li, H., Chen, X., Calhoun-Davis, T., Claypool, K., and Tang, D.G. (2008). PC3 human prostate carcinoma cell holoclones contain self-renewing tumor-initiating cells. Cancer Res. *68*, 1820–1825.

Liu, C., Kelnar, K., Liu, B., Chen, X., Calhoun-Davis, T., Li, H., Patrawala, L., Yan, H., Jeter, C., Honorio, S., et al. (2011). The microRNA miR-34a inhibits prostate cancer stem cells and metastasis by directly repressing CD44. Nat. Med. *17*, 211–215.

Maitland, N.J., Frame, F.M., Polson, E.S., Lewis, J.L., and Collins, A.T. (2011). Prostate cancer stem cells: do they have a basal or luminal phenotype? Horm Cancer *2*, 47–61.

Memarzadeh, S., Cai, H., Janzen, D.M., Xin, L., Lukacs, R., Riedinger, M., Zong, Y., DeGendt, K., Verhoeven, G., Huang, J., and Witte, O.N. (2011). Role of autonomous androgen receptor signaling in prostate cancer initiation is dichotomous and depends on the oncogenic signal. Proc. Natl. Acad. Sci. USA *108*, 7962–7967.

Mostaghel, E.A., Page, S.T., Lin, D.W., Fazli, L., Coleman, I.M., True, L.D., Knudsen, B., Hess, D.L., Nelson, C.C., Matsumoto, A.M., et al. (2007). Intraprostatic androgens and androgen-regulated gene expression persist after testosterone suppression: therapeutic implications for castration-resistant prostate cancer. Cancer Res. *67*, 5033–5041.

Niu, Y., Altuwaijri, S., Lai, K.P., Wu, C.T., Ricke, W.A., Messing, E.M., Yao, J., Yeh, S., and Chang, C. (2008). Androgen receptor is a tumor suppressor and proliferator in prostate cancer. Proc. Natl. Acad. Sci. USA *105*, 12182–12187.

Patrawala, L., Calhoun, T., Schneider-Broussard, R., Zhou, J., Claypool, K., and Tang, D.G. (2005). Side population is enriched in tumorigenic, stem-like cancer cells, whereas ABCG2^{+} and ABCG2^{-} cancer cells are similarly tumorigenic. Cancer Res. *65*, 6207–6219.

Patrawala, L., Calhoun, T., Schneider-Broussard, R., Li, H., Bhatia, B., Tang, S., Reilly, J.G., Chandra, D., Zhou, J., Claypool, K., et al. (2006). Highly purified CD44^{+} prostate cancer cells from xenograft human tumors are enriched in tumorigenic and metastatic progenitor cells. Oncogene *25*, 1696–1708.

Patrawala, L., Calhoun-Davis, T., Schneider-Broussard, R., and Tang, D.G. (2007). Hierarchical organization of prostate cancer cells in xenograft tumors: the CD44$^{+}\alpha2\beta1^{+}$ cell population is enriched in tumor-initiating cells. Cancer Res. *67*, 6796–6805.

Pece, S., Tosoni, D., Confalonieri, S., Mazzarol, G., Vecchi, M., Ronzoni, S., Bernard, L., Viale, G., Pelicci, P.G., and Di Fiore, P.P. (2010). Biological and molecular heterogeneity of breast cancers correlates with their cancer stem cell content. Cell *140*, 62–73.

Rajasekhar, V.K., Studer, L., Gerald, W., Socci, N.D., and Scher, H.I. (2011). Tumour-initiating stem-like cells in human prostate cancer exhibit increased NF-κB signalling. Nat Commun *2*, 162.

Roudier, M.P., True, L.D., Higano, C.S., Vesselle, H., Ellis, W., Lange, P., and Vessella, R.L. (2003). Phenotypic heterogeneity of end-stage prostate carcinoma metastatic to bone. Hum. Pathol. *34*, 646–653.

Ruizeveld de Winter, J.A., Janssen, P.J., Sleddens, H.M., Verleun-Mooijman, M.C., Trapman, J., Brinkmann, A.O., Santerse, A.B., Schröder, F.H., and van der Kwast, T.H. (1994). Androgen receptor status in localized and locally progressive hormone refractory human prostate cancer. Am. J. Pathol. *144*, 735–746.

Ryan, C.J., Smith, A., Lal, P., Satagopan, J., Reuter, V., Scardino, P., Gerald, W., and Scher, H.I. (2006). Persistent prostate-specific antigen expression after neoadjuvant androgen depletion: an early predictor of relapse or incomplete androgen suppression. Urology *68*, 834–839.

Shah, R.B., Mehra, R., Chinnaiyan, A.M., Shen, R., Ghosh, D., Zhou, M., Macvicar, G.R., Varambally, S., Harwood, J., Bismar, T.A., et al. (2004). Androgen-independent prostate cancer is a heterogeneous group of diseases: lessons from a rapid autopsy program. Cancer Res. *64*, 9209–9216.

Shen, M.M., and Abate-Shen, C. (2010). Molecular genetics of prostate cancer: new prospects for old challenges. Genes Dev. *24*, 1967–2000.

Tang, D.G. (2012). Understanding cancer stem cell heterogeneity and plasticity. Cell Res. *22*, 457–472.

Tomlins, S.A., Mehra, R., Rhodes, D.R., Cao, X., Wang, L., Dhanasekaran, S.M., Kalyana-Sundaram, S., Wei, J.T., Rubin, M.A., Pienta, K.J., et al. (2007). Integrative molecular concept modeling of prostate cancer progression. Nat. Genet. *39*, 41–51.

van den Hoogen, C., van der Horst, G., Cheung, H., Buijs, J.T., Lippitt, J.M., Guzmán-Ramírez, N., Hamdy, F.C., Eaton, C.L., Thalmann, G.N., Cecchini, M.G., et al. (2010). High aldehyde dehydrogenase activity identifies tumor-initiating and metastasis-initiating cells in human prostate cancer. Cancer Res. *70*, 5163–5173.

Varambally, S., Yu, J., Laxman, B., Rhodes, D.R., Mehra, R., Tomlins, S.A., Shah, R.B., Chandran, U., Monzon, F.A., Becich, M.J., et al. (2005). Integrative genomic and proteomic analysis of prostate cancer reveals signatures of metastatic progression. Cancer Cell *8*, 393–406.

Wang, Q., Li, W., Zhang, Y., Yuan, X., Xu, K., Yu, J., Chen, Z., Beroukhim, R., Wang, H., Lupien, M., et al. (2009a). Androgen receptor regulates a distinct transcription program in androgen-independent prostate cancer. Cell *138*, 245–256.

Wang, X., Kruithof-de Julio, M., Economides, K.D., Walker, D., Yu, H., Halili, M.V., Hu, Y.P., Price, S.M., Abate-Shen, C., and Shen, M.M. (2009b). A luminal epithelial stem cell that is a cell of origin for prostate cancer. Nature *461*, 495–500.

Wu, M., Kwon, H.Y., Rattis, F., Blum, J., Zhao, C., Ashkenazi, R., Jackson, T.L., Gaiano, N., Oliver, T., and Reya, T. (2007). Imaging hematopoietic precursor division in real time. Cell Stem Cell *1*, 541–554.

Yoshida, T., Kinoshita, H., Segawa, T., Nakamura, E., Inoue, T., Shimizu, Y., Kamoto, T., and Ogawa, O. (2005). Antiandrogen bicalutamide promotes tumor growth in a novel androgen-dependent prostate cancer xenograft model derived from a bicalutamide-treated patient. Cancer Res. *65*, 9611–9616.

Yu, D., Chen, D., Chiu, C., Razmazma, B., Chow, Y.H., and Pang, S. (2001). Prostate-specific targeting using PSA promoter-based lentiviral vectors. Cancer Gene Ther. *8*, 628–635.